Perturbation of Tryptophan Residues by Point Mutations in Bacteriophage T4 Lysozyme Studied by Optical Detection of Triplet-State Magnetic Resonance Spectroscopy†

Li-Hsin Zang, Sanjib Ghosh, and August H. Maki*
Department of Chemistry, University of California, Davis, California 95616
Received September 8, 1988; Revised Manuscript Received November 2, 1988

ABSTRACT: We have investigated perturbations of the triplet-state properties of Trp residues in bacteriophage T4 lysozyme caused by point mutations using low-temperature phosphorescence and optical detection of triplet-state magnetic resonance (ODMR) spectroscopy. Five temperature-sensitive mutants have been studied in detail. These include lysozymes with the point mutations Gln-105 → Ala, Gln-105 → Gly, Gln-105 → Glu, Ala-146 → Thr, and Trp-126 → Gln. Changes in phosphorescence 0,0 band wavelength, intensity, the triplet-state zero-field splitting (ZFS), and the wavelength dependence of the ZFS were detected only from Trp-138 in each mutant. In the case of the Q105A mutation, the perturbations on Trp-138 have been ascribed to the combination of an increase in the polarizability of the environment and to the loss of hydrogen bonding of the enamine nitrogen of indole. For the Q105G mutation, we believe that Q is replaced by a solvent molecule in H bonding, leading to relatively small changes. In the Q105E mutation, the perturbation results largely from the introduction of a charged residue. In the case of the mutation A146T, the perturbation is associated with a local conformational change in which Trp-138 is shifted to a more solvent-exposed location. On the other hand, no significant spectroscopic changes in Trp-126 and Trp-158 were found in any of the mutants, suggesting that the perturbations are probably localized near Trp-138 for the mutations of positions 105 and 146. However, in the mutation W126Q, which occurs ~16 Å away from Trp-138, significant changes of Trp-138 are detected, suggesting that the effects of this mutation are propagated over large distances.

Lysozyme from bacteriophage T4 (T4 lysozyme)[1] has been used as a model to determine the factors which influence the stability and folding of proteins, since the crystal structure of the enzyme is known and various kinds of mutants have been obtained by classical selection as well as by site-directed mutagenesis (Streisinger et al., 1961, 1966; Alber et al., 1986, 1987a,b; Perry & Wetzel, 1984, 1986, 1987). A series of temperature-sensitive mutants whose thermostability or enzymatic activity is substantially altered by changes in a single amino acid have been studied recently by crystallographic and thermodynamic methods (Hawkes et al., 1984; Alber et al., 1986; Grütter et al., 1979, 1987; Gray & Matthews, 1987). It has been reported that the thermally stable proteins are structurally very similar to their less stable homologues. Therefore, it has been suggested that specific noncovalent interactions, such as hydrogen bonds and solvent structure changes, may be responsible for the observed change of a protein's thermal stability (Grütter et al., 1979, 1987). In other work, T4 lysozyme and some of its mutants have been investigated using fluorescence techniques by probing the Trp residues in particular, to determine any changes of the excited-state properties caused by local environmental changes (Harris et al., 1988). Also, changes of the intrinsic fluorescence of Trp residues in T4 lysozyme have been used to study enzyme–inhibitor binding (Vedenkina et al., 1984).

T4 lysozyme contains three Trp residues at positions 126, 138, and 158. The three-dimensional structures of the wild-type enzyme and several temperature-sensitive mutants have been determined (Remington et al., 1978; Weaver & Matthews, 1987; Grütter et al., 1979, 1987; Alber et al., 1986; Gray & Matthews, 1987). The triplet-state spectral and kinetic properties of the individual Trp residues have been characterized using low-temperature phosphorescence and optically detected magnetic resonance (ODMR) spectroscopy of Trp → Tyr double-point mutants which contain only a single Trp residue (Ghosh et al., 1988; Zang et al., 1988).

In this paper, we describe the spectroscopically detected perturbations of Trp residues caused by the single-point mutations in five temperature-sensitive mutants. We find that the triplet state of Trp-138 is selectively perturbed when each of two nearby residues, 105 and 146, is replaced by different amino acids. Furthermore, we report experiments that demonstrate the special interactions between Trp-138 and the residue at position 105 by different mutants in which Gln-105 is replaced by the residues Ala, Gly, and Glu. Significant phosphorescence shifts, changes in the zero-field splitting (ZFS) parameters, and/or the wavelength-dependent pattern of the zero-field splittings (ZFS) of Trp-138 were observed in these mutants and the one in which Ala-146 is replaced by Thr. On the other hand, no significant spectroscopic changes were detected from Trp-126 and -158 in any of these mutants, suggesting that the perturbations from the mutations at positions 105 and 146 are relatively localized. In contrast, the replacement of Trp-126 with Gln changes the wavelength-dependent pattern of the ZFS of Trp-138 even though the mutation occurs about 16 Å away from Trp-138, indicating a long-range propagation to the neighborhood of the active site.

Materials and Methods

The bacteriophage T4 lysozyme mutants studied in this work were generous gifts from Professor B. W. Matthews, L. McIntosh, and co-workers, Institute of Molecular Biology,

† This work was supported by a NSF grant.

[1] Abbreviations: *D* and *E*, triplet-state zero-field splitting parameters; ODMR, optical detection of triplet-state magnetic resonance; T4 lysozyme, bacteriophage T4 lysozyme; ZFS, triplet-state zero-field splitting(s).

0006-2960/89/0428-2245$01.50/0

Table I: Phosphorescence 0,0 Band Maxima and Phosphorescence Lifetimes of Trp Residues in Wild-Type and Various Mutated Enzymes

system[a]	$\lambda_{0,0}$ (nm)[b]	λ_{em} (nm)[b]	lifetime components (s)
WWW[c]	407.8	408.4	1.15 (25%), 6.28 (75%)
	413.5	414.0	1.18 (30%), 5.61 (70%)
Q105A	407.2	407.2	0.82 (23%), 6.33 (77%)
	417.2	417.2	0.625 (21%), 5.51 (79%)
Q105G	407.1	407.1	1.53 (13%), 6.43 (87%)
	413.3	413.3	1.72 (20%), 5.87 (80%)
Q105E	407.1	407.1	2.11 (5%), 6.49 (95%)
	413.1	413.1	2.83 (18%), 6.09 (82%)
A146T	409.7	410.0	2.75 (29%), 6.11 (71%)
		412.0	2.65 (32%), 5.81 (68%)
W126Q	408.1	409.0	1.14 (34%), 6.14 (66%)
	412.9	413.4	1.20 (41%), 5.15 (59%)

[a] Measurements were made at 77 K. The excitation was at 295 nm with a 16-nm bandwidth for all the samples except W126Q which was excited at 305 nm with the same bandwidth. [b] $\lambda_{0,0}$ is the peak wavelength of the corresponding 0,0 band; λ_{em} is the monitored wavelength at which decay is measured using 1-nm bandwidth. [c] Data from Ghosh et al. (1988).

Eugene, OR. The proteins were stored in 100 mM sodium phosphate buffer containing ca. 500 mM NaCl and 0.01% NaN_3 at 4 °C. Before spectroscopic measurements were made, 10 mM dithiothreitol was added to the protein stock solution to prevent oxidation of cysteine residues; 30% glycerol (v/v) was then added to the protein solution as a cryogenic solvent.

For consistency in terminology with previous work (Ghosh et al., 1988), WWW and YWY are used to designate the wild-type enzyme (indicating Trp-126, -138, and -158) and a double-point mutant with two Trp → Tyr substitutions (indicating Tyr-126, Trp-138, and Tyr-158), respectively. The five temperature-sensitive mutants studied are named Q105A, Q105G, Q105E (mutation of Gln-105 to Ala, Gly, and Glu, respectively), A146T (mutation of Ala-146 to Thr), and W126Q (mutation of Trp-126 to Gln).

The ODMR apparatus and experimental methods of phosphorescence and ODMR slow passage have been described previously (Ghosh et al., 1984).

Results

Phosphorescence Spectra. The phosphorescence spectra of Trp residues in WWW, Q105A, Q105E, Q105G, A146T, and W126Q at 4.2 K are shown in Figure 1. The wavelengths of the corresponding 0,0 bands of each sample are presented in Table I. Previous studies have demonstrated that the two well-resolved 0,0 bands of WWW, which peak at 407.8 and 413.8 nm, originate from Trp-158 and -138, respectively; the emission of Trp-126 is largely quenched by efficient selective singlet–singlet energy transfer to Trp-158 (Ghosh et al., 1988). Comparison of the spectra (Figure 1) shows that the 0,0 band originating from Trp-138 is red-shifted by about 4 nm in Q105A relative to WWW. Crystallographic analysis has shown that this mutation eliminates the hydrogen bond between the enamine nitrogen atom of Trp-138 and the side chain carbonyl of Gln-105 (L. McIntosh et al., unpublished results). The replacement of the neighboring Gln-105 with Ala increases the overall polarizability of the Trp-138 environment, which leads to a red shift of its phosphorescence. In addition, the loss of the hydrogen bond destabilizes the ground state of Trp-138 relative to the lowest triplet excited state, contributing to a red shift in the phosphorescence spectrum. In contrast, the 0,0 band of Trp-138 is blue-shifted in A146T where the mutation introduces a bulkier alkyl group at position 146. The blue shift of Trp-138 results in considerable overlap

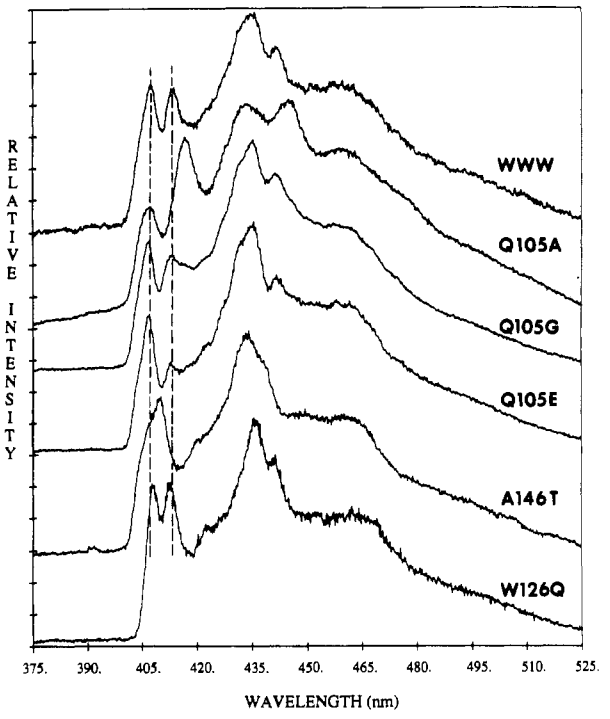

FIGURE 1: Phosphorescence spectra of wild-type T4 lysozyme WWW and its temperature-sensitive mutants Q105A, Q105G, Q105E, A146T, and W126Q in phosphate buffer containing 30% glycerol at 4.2 K with emission monochromator resolution of 1.5 nm. Excitation wavelength was 295 nm with 16-nm band pass. The protein concentrations are ca. (1–2) × 10^{-4} M.

of the 0,0 bands of these residues (Figure 1). On the other hand, although the 0,0 band of Trp-138 in Q105G and Q105E does not exhibit a significant shift, a reduction of the phosphorescence intensity is observed in each protein, and the 0,0 band of Trp-138 in Q105G is somewhat broadened. The mutation of Trp-126 to Gln, which is almost 16 Å away, shows much less influence on the phosphorescence of Trp-138 (with only a 0.6-nm blue shift). However, the ODMR measurements, described in a later section, reveal a rather large change in the wavelength dependence of the ZFS of Trp-138, as well as shifts in the ZFS parameters.

The spectra compared in Figure 1 also show that the 0,0 band originating from Trp-158 does not undergo dramatic changes in any mutant enzyme. The ODMR results which are discussed later also show that the triplet-state properties of Trp-158 in each mutant remain nearly the same, which demonstrates that Trp-138 is perturbed selectively by these mutations.

The phosphorescence lifetime of each Trp residue in these mutants was measured at 77 K, monitoring the corresponding 0,0 bands. The lifetimes are given in Table I. Two exponential components were obtained from the computer analysis. The short-lived component (1–2 s) is due to the contribution of tyrosine phosphorescence which has a broad emission band with a maximum at ca. 400 nm. Previous studies (Zang et al., 1988) on mutants containing a single Trp residue show that Trp-138, which is buried in a hydrophobic environment, has a shorter lifetime (~5.6 s) than Trp-158 and Trp-126 (~6.3 s), which are solvent-exposed residues. The decay lifetimes of Trp-138 in Q105G and in Q105E are significantly longer than that in the wild-type enzyme, WWW, whereas the lifetime of Trp-138 in W126Q is slightly shorter than that in WWW. Only small changes in the Trp-138 lifetime are caused by the mutations Q105A and A146T. The phosphorescence lifetimes of Trp-158 in all the mutants are the

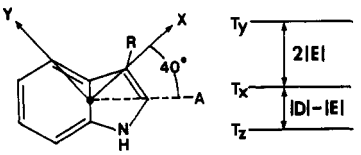

FIGURE 2: Molecular axes convention and triplet sublevel splittings of Trp in zero field.

Table II: Zero-Field Splitting Parameters of Trp Residues in the Wild-Type T4 Lysozyme and Several of Its Mutants

system	λ_{em} (nm)[a]	$\|D\| - \|E\|$ (GHz)[b]	$2\|E\|$ (GHz)[b]	$\|D\|$ (GHz)	$\|E\|$ (GHz)
WWW[c]	407.8	1.78	2.47	3.01	1.24
	413.6	1.625	2.695	2.975	1.350
YWY[c]	413.5	1.630 (40)	2.690 (50)	2.970	1.345
Q105A	407.1	1.78	2.48	3.01	1.24
	417.2	1.575 (40)	2.720 (80)	2.930	1.360
Q105G	407.0	1.78	2.48	3.02	1.24
	413.3	1.625 (40)	2.710 (80)	2.980	1.355
Q105E	407.1	1.78	2.47	3.02	1.24
	413.1	1.640 (45)	2.760 (65)	3.020	1.380
A146T	407.4	1.78	2.47	3.02	1.24
	411.0	1.685 (90)	2.600 (120)	2.985	1.300
W126Q	408.0	1.77	2.48	3.01	1.24
	413.0	1.640 (35)	2.705 (70)	2.990	1.350

[a] Peaks of the phosphorescence 0,0 band were monitored in all proteins except A146T in which emission was monitored at the blue and red edge of its composite 0,0 band, respectively. [b] Measured at 1.2 K with ±5-MHz accuracy for the red-shifted peak which is assigned to Trp-138 and with ±10-MHz accuracy for the blue-shifted peak which is assigned to Trp-158. Full width of the transitiion at half-maximum in megahertz appears in parentheses. Both transition frequency and line width have been extrapolated to zero microwave sweep rate. [c] Data from Ghosh et al. (1988).

same within the experimental error (±0.1 s).

ODMR Transitions. In order to determine the effects on the triplet-state ZFS of Trp-138, which undergoes readily measurable changes in the phosphorescence 0,0 band wavelengths and the lifetime, ODMR slow-passage measurements were conducted by monitoring the phosphorescence at the peak of the 0,0 band of Trp-138. The ODMR of Trp-158 was obtained by monitoring its 0,0 band. In the case of A146T where the 0,0 band of Trp-138 overlaps to a large extent with that of Trp-158, the measurements were made by monitoring at the blue edge or the red edge of the composite band. The energy level diagram and molecular axes convention of tryptophan are shown in Figure 2, and the ODMR spectra corresponding to Trp-138 are shown in Figure 3. The ODMR transitions and corresponding ZFS parameters of the Trp residues in each mutant are presented in Table II. The ZFS of each Trp residue in T4 lysozyme has been isolated by using the three mutants which contain two Trp → Tyr substitutions (Ghosh et al., 1988). These results have shown that Trp-126 and Trp-158 have similar D and E values, while Trp-138 gives a quite different ZFS. The D and E values of Trp-138 in WWW (Table II) are lower and higher, respectively, than those of Trp-158 and Trp-126, indicating (Hershberger et al., 1980) that the latter residues are located in a more polar environment. Furthermore, the ODMR transition line widths for Trp-138 are much narrower than those obtained from Trp-126 and Trp-158, which indicates that Trp-138 is located in a relatively homogeneous environment (Maki, 1984; Davis & Maki, 1984). These experimental observations may be interpreted with regard to the local environments of Trp residues in T4 lysozyme and are consistent with the crystal structure results (Remington et al., 1978; Weaver & Matthews, 1987) which indicate that Trp-138 is a buried residue while Trp-126 and -158 are solvent exposed.

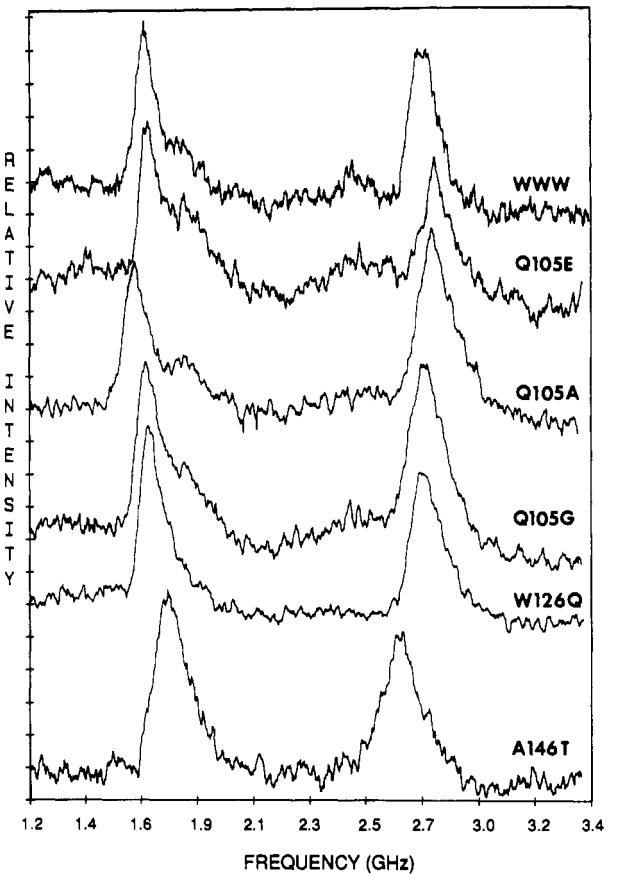

FIGURE 3: Slow-passage ODMR transitions of Trp-138 in WWW and in five mutants at 1.2 K. Measurements were done by monitoring at the peak of the 0,0 band of Trp-138 in each sample with 1.5-nm bandwidth, except in A146T where the emission was monitored at 411.0 nm. The microwave sweep rate was 58 MHz/s.

Comparison of the data presented in Table II shows that the D and E values of Trp-138 in Q105A are shifted further to lower and high frequencies, respectively, than those of Trp-138 in WWW or YWY, while the ODMR transition line widths remain narrow. This indicates that Trp-138 in Q105A continues to experience a homogeneous environment after the mutation of Gln to Ala, and it still remains buried. In accord with the opposite direction of the phosphorescence shift of Trp-138 in A146T relative to Q105A, the D and E values now shift oppositely, as well, namely to higher and lower frequencies, respectively. Moreover, the ODMR transition line widths of Trp-138 in A146T are significantly broader than those in WWW and in the other mutants (Table II). Both these effects, namely, an increase in $|D| - |E|$ and in the ODMR line width, have been associated with increasing exposure of the Trp residue to the polar solvent [see Maki (1984) and references cited therein]. These observations suggest that the Trp-138 in A146T has been moved out of the hydrophobic environment which it occupies in WWW and in Q105A, into a more solvent-exposed position. In Q105E in which the mutation replaces Gln by a charged group Glu, even though the phosphorescence 0,0 band of Trp-138 remains unshifted, a considerable change in the ZFS is observed. Both the D and E values are larger than those of Trp-138 in WWW, but no significant changes in the transition line widths are observed. Therefore, the change of the ZFS of Trp-138 in Q105E may be attributed to a uniform Stark effect induced by the negatively charged group introduced by the mutation. The mutation of Trp-126 to Gln in W126Q is not close to Trp-138; on the other hand, the substitution severely reduced the thermal stability of the protein (L. McIntosh, personal com-

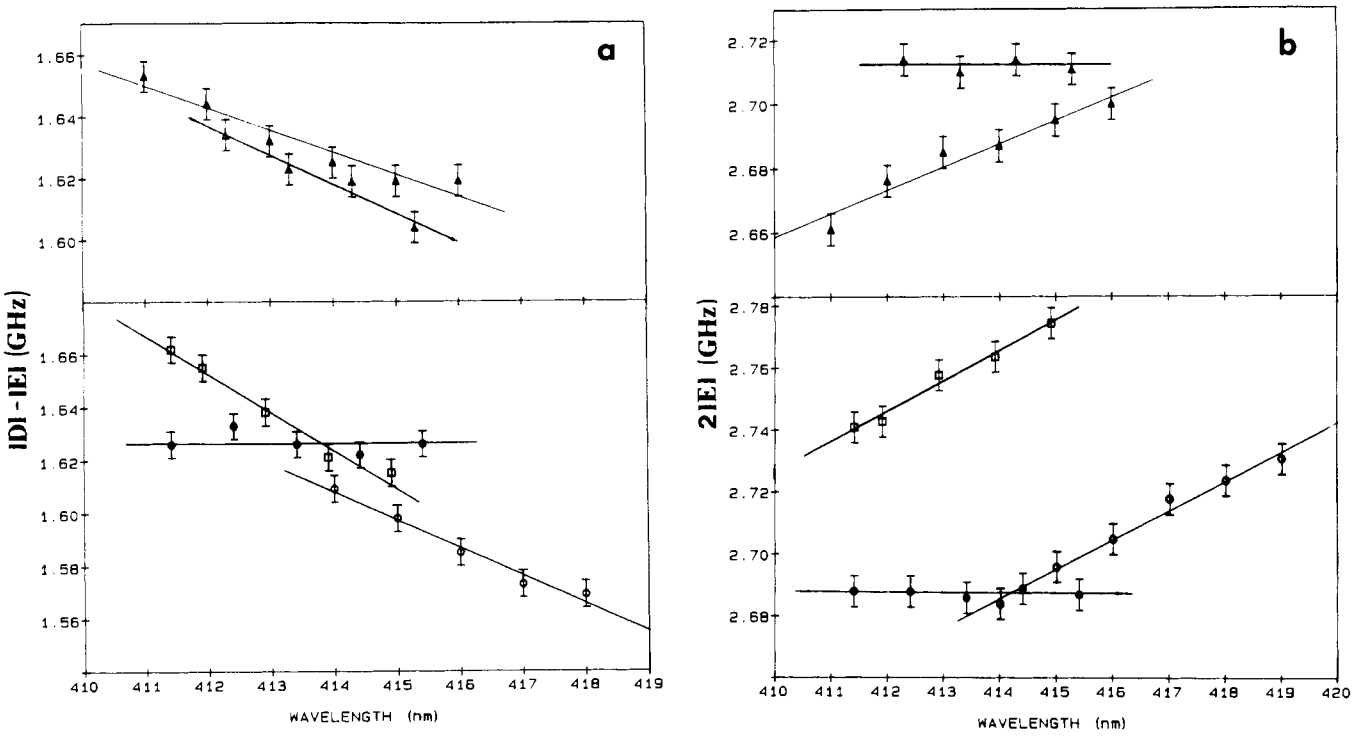

FIGURE 4: Plot of (a) the $|D| - |E|$ and (b) the $2|E|$ ODMR transition frequency vs emission wavelength through the 0,0 band region of Trp-138 in YWY (●), Q105A (○), Q105E (□), Q105G (△), and W126Q (▲). The microwave sweep rate in each case was 58 MHz/s. The temperature was 1.2 K, and the emission bandwidth was 1 nm. The transition frequencies were all corrected for rapid-passage effects.

munication). We find from ODMR measurements that a moderate increase of the D value of Trp-138 occurs in W126Q. It is very interesting that unlike Q105A, Trp-138 in Q105G does not show a large change in the ZFS, although this mutation also lacks a hydrogen bond between Trp-138 and the residue at position 105. Both the D and E values are only very slightly increased. It has been found from the crystal structure of Q105G (B. W. Matthews, personal communication) that the much smaller residue Gly leaves enough room for a H_2O molecule to occupy the Gln side chain position. Consequently, a hydrogen bond formed between Trp-138 and the internal H_2O compensates for the increase in energy caused by the solvent rearrangement. Therefore, it is not surprising that the ZFS of Trp-138 in Q105G does not undergo a significant change. The solvent effect of a hydrogen-bonded H_2O molecule effectively mimics that of the native Gln-site chain. Our results, obtained from both phosphorescence and ODMR, are consistent with the X-ray study of Q105G, suggesting that the Trp-138 environment in a 30% glycerol matrix at low temperature contains a H_2O molecule in the Q105 cavity and thus is similar to that in the crystalline enzyme.

The D and E values obtained for Trp-126 and -158 in all the temperature-sensitive mutants are similar to those found in the wild-type enzyme (Table II), which implies, along with the phosphorescence spectra and lifetime studies, that these environments are not changed significantly in the Q105 and A146 mutants.

Wavelength-Selected ODMR Measurements. In order to further define the perturbations on Trp-138 caused by these mutations, we carried out wavelength-selected ODMR measurements, in which the ZFS was measured by monitoring different wavelengths across the 0,0 band corresponding to Trp-138. The results are plotted with the transition frequencies given vs monitored wavelengths in Figures 4 and 5. Unlike the results for Trp-138 in YWY where both $|D| - |E|$ and $2|E|$ transition frequencies are wavelength independent (Ghosh et al., 1988), a linear wavelength dependence of the $|D| - |E|$ and

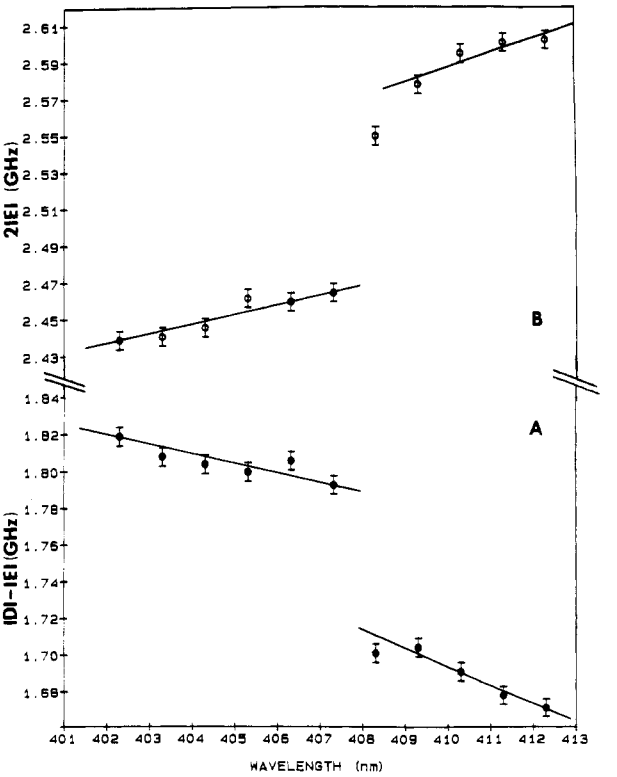

FIGURE 5: Plot of (A) the $|D| - |E|$ and (B) the $2|E|$ ODMR transition frequency vs emission wavelength across the 0,0 band region in A146T. The transition frequencies were corrected for rapid-passage effects. Other conditions are the same as described in the Figure 3 caption.

$2|E|$ frequencies was obtained for the Trp-138 in Q105A, Q105E, W126Q (Figure 4), and A146T (Figure 5). In the case of Q105G, wavelength-independent $2|E|$ but wavelength-dependent $|D| - |E|$ frequencies were observed. The measurements made for Q105A, Q105G, and W126Q are relatively more accurate, since the phosphorescence 0,0 band

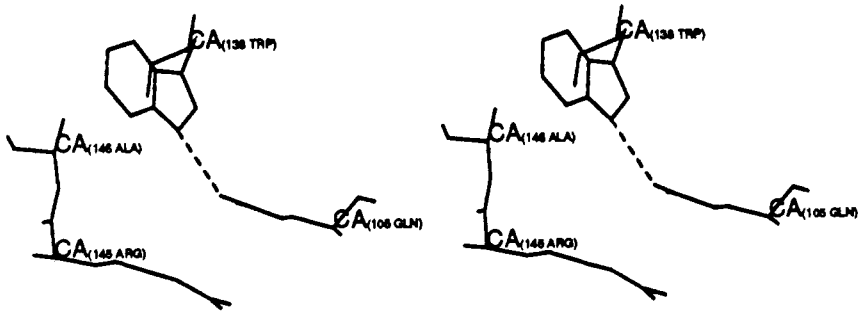

FIGURE 6: Stereoview drawing showing the vicinity of Trp-138 in the wild-type T4 lysozyme. The distance between $N_{\eta 1}$ of Arg-145 and $N_{\epsilon 2}$ of Gln-105 is 3.94 Å, and that between $N_{\epsilon 1}$ of Trp-138 and $O_{\epsilon 1}$ of Gln-105 is 2.81 Å.

of Trp-138 is well resolved. However, in A146T, the blue-shifted 0,0 band of Trp-138 overlaps severely with that of Trp-158. Therefore, the measurements were done by monitoring different wavelengths across the composite band. In spite of the phosphorescence overlap, the two Trp sites were clearly resolved in the plot of ODMR frequency vs monitored wavelength (Figure 5), in which the discontinuities result from the different transition frequencies of Trp-138 relative to those of Trp-158 and -126 (Table II). The results show that the ZFS of both Trp-138 and Trp-158 are wavelength dependent, supporting the conclusion that Trp-138 in A146T experiences a more solvent-exposed environment. It is particularly interesting that Trp-138 for Q105G has a wavelength-dependent $|D| - |E|$ transition but that the $2|E|$ transition is wavelength independent, which means that the D value depends linearly on the wavelength instead of the E value as occurs in most other cases.

A model of the molecule–solvent electric field (Stark) interaction based on the spin–spin dipolar coupling predicts a linear wavelength dependence of the ZFS parameters on the phosphorescence wavelength (van Egmond et al., 1975; Gradl et al., 1986). Generally, in proteins this linear dependence of the ZFS may occur either in a solvent-exposed probe or in a buried one. However, some sites are found which exhibit very little correlation between the environmental-induced Stark shift and the ZFS parameters. In fact, this lack of wavelength dependence of the ZFS has been observed only in buried Trp residues (Hershberger et al., 1980; Davis & Maki, 1984). As demonstrated in earlier work (Ghosh et al., 1988), Trp-138 in wild-type T4 lysozyme exhibits wavelength-independent ZFS while that of Trp-126 is wavelength dependent. The introduction of a wavelength-dependent pattern for the ZFS of Trp-138 in all the temperature-sensitive mutants may result either from Trp-138 being shifted to a more solvent-exposed environment or from changes in the local electric field resulting from displacement and/or introduction of charged groups.

Discussion

Trp-138 in T4 lysozyme is a buried residue near the active site. The crystal structure shows that the nearby Gln-105 forms a hydrogen bond with the N–H of the indole ring (Remington et al., 1978; Weaver & Matthews, 1987). In the three Q105X (X = A, G, E) mutants, Ala, Gly and Glu, respectively, replace Gln-105. This set of mutants provides a unique opportunity to investigate changes of the triplet-state properties of Trp-138 which are induced by the changes at a single position. Aside from the solvent rearrangement in Q105G, very little structural change has been detected by X-ray studies in these Q105X mutants (B. W. Matthews, personal communication). However, rather large perturbations of the Trp-138 triplet state have been observed from our spectroscopic measurements. First of all, among all three Q105X mutants, a large red shift of the 0,0 band of Trp-138 appears only in Q105A. We cannot determine quantitatively how much of this shift is due to the increased polarizability of the environment and how much is due to the loss of the hydrogen bond. Since there probably is little difference in polarizability between Ala and Gln, we think polarizability effects are of smaller consequence. If this is the case, we can conclude that hydrogen bonding of the indole N–H stabilizes the ground electronic state more than it does the triplet state. On the other hand, retention of a hydrogen bond with the N–H of the indole ring of Trp-138 in Q105G and Q105E results in relatively minor changes in the triplet-state energy relative to that in WWW. Although the 0,0 band of Trp-138 in these two mutant enzymes remains unshifted, different peak intensities as well as changes in the phosphorescence lifetime and the ZFS of Trp-138 were observed. We may conclude that the hydrogen bonds between Trp-138 and H_2O in Q105G, between Trp-138 and Glu-105 in Q105E, and between Trp-138 and Gln-105 in WWW are different in terms of their effects on the photophysics of Trp-138 and on the electron dipolar coupling of its triplet state. When the negatively charged Glu replaces Gln, the phosphorescence intensity of Trp-138 decreases dramatically, while the phosphorescence lifetime becomes longer than that in WWW. Moreover, the D and E values of Trp-138 both increase, and a linear wavelength dependence of the ZFS is produced. The changes in the local electric field and, to a small extent, the polarizability of the local environment of Trp-138 seem to be responsible for the perturbation of the triplet state of Trp-138 in Q105E. As suggested by the crystal structure of the wild-type enzyme (Figure 6), a stronger hydrogen bond may form between the N–H of Trp-138 and $CO^{\delta-}$ of Glu-105, and the adjacent positively charged Arg-145 may form an internal salt bridge with this negatively charged residue in Q105E. It is possible that the introduction of such a salt bridge leads to fluorescence quenching via exciplex formation, resulting in a reduction of the phosphorescence quantum yield. Changes observed in the ZFS of Trp-138 arise from Stark shifts induced by local changes in the electric field. Previous studies (Lemaistre & Zewail, 1979; Clark & Tinti, 1979; van Egmond et al., 1975) have resulted in two proposed mechanisms for electric field modification of ZFS, namely, spin–orbit interactions and electric field induced mixing of triplet states. The model based on spin–orbit coupling (Lemaistre & Zewail, 1979) does not apply to tryptophan because it is valid only for those molecules whose ZFS results to a large extent from the spin–orbit interaction in the first place (Maki, 1984). Since Trp has a long triplet-state lifetime, spin–orbit effects are minimal, and it is most likely that the local electric fields which mix higher triplet states with the phosphorescent state are responsible for the shifts of the D and E values through alteration of the spin–spin dipolar coupling. The electric field effects on the dipolar

coupling give rise to the wavelength dependence of the ZFS when Gln-105 is substituted by a negatively charged Glu. Electric field effects on the ZFS of Trp have been observed previously. It has been reported that when porcine pancreatic phospholipase A2 binds to a negatively charged lipid substrate, a large reduction of the E value of Trp results (Mao et al., 1986), which was explained by the postulated location of perturbing electrical charges within the indole plane. Such a location of charged groups would perturb primarily the E value (Maki, 1984). In T4 lysozyme, however, we find that D and E are both increased when Gln-105 is substituted by Glu. It should be noted that Arg-145, a positively charged group, is located roughly within the indole plane of Trp-138 and ca. 6 Å from the edge of the indole in the wild-type enzyme (Figure 6). This charged residue probably contributes significantly to the ZFS pattern in the wild-type enzyme. The mutation of Gln-105 to the negatively charged Glu may reduce significantly the electric field generated at Trp-138 by Arg-145 through the formation of an internal salt bridge. Because of the unsymmetrical location of the resulting dipole with respect to the indole plane of Trp-138, the observed changes in both D and E are reasonable. In Q105G, the unshifted phosphorescence 0,0 band of Trp-138 and its slight broadening are in accord with the crystal structure, where a H_2O molecule hydrogen bonded to the indole N–H of Trp-138 is found situated in the pocket created by the mutation. The direction of the ZFS shift of Trp-138 is the same as that in Q105E, but it occurs with much smaller amplitude; the D and E values both are only slightly increased. This suggests that the local electric field produced by H_2O is similar to that of Gln in WWW; hence, the perturbation on the ZFS is considerably less than that which occurs with the Gln to Glu mutation. Finally, the ODMR signal line widths of Trp-138 remain relatively narrower than those of Trp-126 and -158 in the three Q105 mutants, further indicating that there is little conformational heterogeneity induced in the vicinity of Trp-138 and that this residue remains buried in a relatively well-defined local environment.

Unlike the Q105 point mutants, in A146T the perturbation of Trp-138 is due mainly to a significant local conformational change induced by the mutation. According to Alber et al. (1986), the substitution of Ala-146, an internal and almost completely solvent-inaccessible residue, with the bulkier Thr displaces neighboring groups, resulting in an outward movement of the indole ring of Trp-138 by about 0.7 Å. Our spectroscopic investigations characterize the perturbations of Trp-138 as a blue shift of the phosphorescence, an increase in D and decrease in E values, and an induced wavelength dependence of the ZFS, all suggesting that the mutation moves Trp-138 into a more solvent-exposed location.

Although there is no structural information available, the change of the D parameter and the wavelength-dependent pattern of the ZFS of Trp-138 induced in W126Q suggest that this perturbation is propagated to the vicinity of Trp-138.

In summary, our investigation of the perturbations of Trp residues in T4 lysozyme induced by point mutations using low-temperature phosphorescence and ODMR spectroscopy reveals that the triplet state of Trp-138 in all five temperature-sensitive mutants is perturbed in various ways and to different extents. Although X-ray studies show that very little structural change of the enzyme accompanies the mutations at position 105 reported in this work, very different triplet-state behaviors of Trp-138 have been observed. The perturbations arise mainly from such effects as the loss of the hydrogen bond, the introduction of a buried H_2O molecule, and the introduction of an electrically charged group, which alters the local electric field. Some changes in the polarizability of the local environment may also be significant. These spectroscopic measurements also demonstrate that local charges and dipoles play an important role in determining the triplet-state properties of the probe Trp and a suggested hierarchy of perturbations is hydrogen bonds $\sim$ local charges > dipole moments > induced dipole moments (related to the polarizability). On the other hand, the mutation which introduces a bulky group at position 146 yields a local conformational change which moves Trp-138, a buried residue in WWW, to a more solvent-exposed environment. This shift of Trp-138 is observed in the crystal structure of the A146T mutant (Alber et al., 1986). Although the mutation at position 126 is not close to either of the remaining Trp residues, small but significant changes of the triplet-state properties of Trp-138 were detected by ODMR techniques.

Acknowledgments

We thank L. McIntosh and J. Wozniak for preparing the temperature-sensitive mutants studied in this work. We also thank Dr. B. W. Matthews for providing some preliminary results of X-ray crystallography and for helpful suggestions concerning this work. We thank the Computer Graphics Laboratory at the University of California, San Francisco, for the use of their facilities.

Registry No. Trp, 73-22-3; lysozyme, 9001-63-2.

References

Alber, T., & Matthews, B. W. (1987) *Protein Eng.*, 289–297.

Alber, T., Grütter, M. G., Gray, T. M., Wozniak, J. A., Weaver, L. H., Chen, B.-L., Baker, E. N., & Matthews, B. W. (1986) in *Protein Structure, Folding, and Design* (Oxender, D. L., Ed.) pp 307–318, Alan R. Liss, Inc., New York.

Alber, T., Dao-Pin, S., Wilson, K., Wozniak, J. A., Cook, S. P., & Matthews, B. W. (1987a) *Nature 330*, 41–46.

Alber, T., Dao-Pin, S., Nye, J. A., Muchmore, D. C., & Matthews, B. W. (1987b) *Biochemistry 26*, 3754–3758.

Clark, S. E., & Tinti, D. S. (1979) *Chem. Phys. Lett. 60*, 292–297.

Davis, J. A., & Maki, A. H. (1984) *Biochemistry 23*, 6249–6256.

Ghosh, S., Weers, J. G., Petrin, M., & Maki, A. H. (1984) *Chem. Phys. Lett. 108*, 87–93.

Ghosh, S., Zang, L.-H., & Maki, A. H. (1988) *J. Chem. Phys. 88*, 2769–2775.

Gradl, G., Friedrich J., & Kohler, B. E. (1986) *J. Chem. Phys. 84*, 2079–2083.

Gray, T. M., & Matthews, B. W. (1987) *J. Biol. Chem. 262*, 16858–16864.

Grütter, M. G., Hawkes, R. B., & Matthews, B. M. (1979) *Nature 277*, 667–669.

Grütter, M. G., Gray, T. M., Weaver, L. H., Alber, T., Wilson, K., & Matthews, B. W. (1987) *J. Mol. Biol. 197*, 315–329.

Harris, D., McIntosh, L., Weaver, L., Gray, T., & Hudson, B. (1988) *Biophys. J. 53*, 47a.

Hawkes, R., Grütter, M. G., & Schellman, J. (1984) *J. Mol. Biol. 175*, 192–212.

Hershberger, M. V., Maki, A. H., & Galley, W. C. (1980) *Biochemistry 19*, 2204–2209.

Lemaistre, J. P., & Zewail, A. H. (1979) *Chem. Phys. Lett. 68*, 296–301.

Maki, A. H. (1984) *Biol. Magn. Reson. 6*, 187–294.

Perry, L. J., & Wetzel, R. (1984) *Science 226*, 555–557.

Perry, L. J., & Wetzel, R. (1986) *Biochemistry 25*, 733–739.

Perry, L. J., & Wetzel, R. (1987) *Protein Eng. 1*, 101–105.
Remington, S. J., Anderson, W. F., Owen, J., Ten Eyck, L. F., Grainger, C. T., & Matthews, B. W. (1978) *J. Mol. Biol. 118*, 81–89.
Streisinger, G., Mukai, F., Dreyer, W. J., Miller, B., & Horiuchi, S. (1961) *Cold Spring Harbor Symp. Quant. Biol. 26*, 25–30.
Streisinger, G., Okada, Y., Emrich, J., Newton, J., Tsugita, A., Terzahi, E., & Inouye, M. (1966) *Cold Spring Harbor Symp. Quant. Biol. 31*, 77–84.
van Egmond, J., Kohler, B. E., & Chan, I. Y. (1975) *Chem. Phys. Lett. 34*, 423–426.
Vedenkina, N. S., Troitskill, A. V., & Burshtein, E. A. (1984) *Mol. Biol. (Engl. Transl.) 18*, 362–369.
Weaver, L. H., & Matthews, B. W. (1987) *J. Mol. Biol. 193*, 189–199.
Zang, L.-H., Ghosh, S., & Maki, A. H. (1988) *Biochemistry 27*, 7820–7825.

Characterization of the Inhibitor Complexes of Cobalt Carboxypeptidase A by Electron Paramagnetic Resonance Spectroscopy†

Richard A. Martinelli,‡ Graeme R. Hanson,§ Jeffery S. Thompson,∥ Barton Holmquist, John R. Pilbrow,⊥ David S. Auld, and Bert L. Vallee*

Center for Biochemical and Biophysical Sciences and Medicine, Harvard Medical School, and Brigham and Women's Hospital, Boston, Massachusetts 02115

Received August 10, 1988; Revised Manuscript Received October 26, 1988

ABSTRACT: The metal coordination sphere of cobalt-substituted carboxypeptidase A and its complexes with inhibitors has been characterized by X-band electron paramagnetic resonance (EPR) spectroscopy. The temperature dependence of the EPR spectrum of cobalt carboxypeptidase and the g anisotropy are consistent with a distorted tetrahedral geometry for the cobalt ion. Complexes with L-phenylalanine, a competitive inhibitor of peptide hydrolysis, as well as other hydrophobic L-amino acids all exhibit very similar EPR spectra described by three g values that differ only slightly from that of the cobalt enzyme alone. In contrast, the EPR spectra observed for the cobalt enzyme complexes with 2-(mercaptoacetyl)-D-Phe, L-benzylsuccinate, and L-β-phenyllactate all indicate an approximately axial symmetry of the cobalt atom in a moderately distorted tetrahedral metal environment. Phenylacetate, β-phenylpropionate, and indole-3-acetate, which exhibit mixed modes of inhibition, yield EPR spectra indicative of multiple binding modes. The EPR spectrum of the putative 2:1 inhibitor to enzyme complex is more perturbed than that of the 1:1 complex. For β-phenylpropionate, partially resolved hyperfine coupling (122×10^{-4} cm^{-1}) is observed on the $g = 5.99$ resonance, possibly indicating a stronger metal interaction for this binding mode. The structural basis for the observed EPR spectral perturbations is discussed with reference to the existing crystallographic kinetic and electronic absorption, nuclear magnetic resonance, and magnetic circular dichroic data.

A detailed description of the catalytic role of the essential active-site zinc ion in carboxypeptidase A (CPD-A)[1] (EC 3.4.17.1) requires an understanding of the alterations in the metal coordination sphere accompanying the binding of ligands. Substitution of the active-site zinc atom in CPD-A with cobalt produces a metallo derivative of the enzyme that is active toward both peptide and depsipeptide substrates (Auld & Holmquist, 1974), and X-ray crystallography has shown crystalline Co(II)CPD to have a metal binding site structure similar to that of the native enzyme (Hardman & Lipscomb, 1984). This metal substitution allows the binding of inhibitors and substrates to be monitored by electronic absorption, MCD, EPR, and NMR spectroscopy (Latt & Vallee, 1971; Holmquist et al., 1975; Vallee & Holmquist, 1980; Geoghegan et al., 1983, 1986; Auld et al., 1984, 1986; Kuo & Makinen, 1985; Makinen et al., 1985; Bertini & Luchinat, 1986; Bertini et al., 1988; Bicknell et al., 1988; Luchinat et al., 1988).

The structural characterization of the complexes of Co(II)CPD with various ligands by spectral means has relied primarily on electronic spectroscopy including absorbance, CD, and MCD. The correlation of the spectral features of the cobalt d–d transitions with overall metal geometry of cobalt complex ions has enabled assignments to be made for cobalt-substituted enzymes (Latt & Vallee, 1971; Holmquist & Vallee, 1978). On this basis, the metal environment in Co(II)CPD and some of its inhibitor complexes have been classified as tetrahedral-like. MCD, a technique that allows

† Supported in part by grants from the Australian Research Grants Scheme. J.S.T. was supported by a postdoctoral fellowship from the American Cancer Society. G.R.H. was a recipient of a Research Fellowship from the Scheme.

‡ Permanent address: Ciba-Corning Diagnostics Corp., 63 North St., Medfield, MA 02052.
§ Permanent address: Department of Chemistry, University of Queensland, St. Lucia, Queensland, Australia 4067.
∥ Permanent address: Central Research and Development Department, E. I. du Pont de Nemours & Co., Experimental Station, Wilmington, DE 19898.
⊥ Permanent address: Physics Department, Monash University, Clayton, Victoria, Australia 3168.

[1] Abbreviations: CPD-A, native zinc carboxypeptidase A; Co(II)-CPD, cobalt substituted carboxypeptidase; apo, metal-free; MCD, magnetic circular dichroism; EPR, electron paramagnetic resonance; CD, circular dichroism; Hepes, *N*-(2-hydroxyethyl)piperazine-*N*′-2-ethanesulfonic acid; Mes, 2-(*N*-morpholino)ethanesulfonic acid; LSE, measure of the least-squares error between the simulated and experimental EPR spectra.

0006-2960/89/0428-2251$01.50/0